ACS Biomaterials SCIENCE & ENGINEERING

Article

pubs.acs.org/journal/abseba

3D Printing of a Double Network Hydrogel with a Compression Strength and Elastic Modulus Greater than those of Cartilage

Feichen Yang, Vaibhav Tadepalli, and Benjamin J. Wiley*

Department of Chemistry, Duke University, Durham, North Carolina 27708, United States

Supporting Information

ABSTRACT: This article demonstrates a two-step method to 3D print double network hydrogels at room temperature with a low-cost ($300) 3D printer. A first network precursor solution was made 3D printable via extrusion from a nozzle by adding a layered silicate to make it shear-thinning. After printing and UV-curing, objects were soaked in a second network precursor solution and UV-cured again to create interpenetrating networks of poly(2-acrylamido-2-methylpropanesulfonate) and polyacrylamide. By varying the ratio of polyacrylamide to cross-linker, the trade-off between stiffness and maximum elongation of the gel can be tuned to yield a compression strength and elastic modulus of 61.9 and 0.44 MPa, respectively, values that are greater than those reported for bovine cartilage. The maximum compressive (93.5 MPa) and tensile (1.4 MPa) strengths of the gel are twice that of previous 3D printed gels, and the gel does not deform after it is soaked in water. By 3D printing a synthetic meniscus from an X-ray computed tomography image of an anatomical model, we demonstrate the potential to customize hydrogel implants based on 3D images of a patient's anatomy.

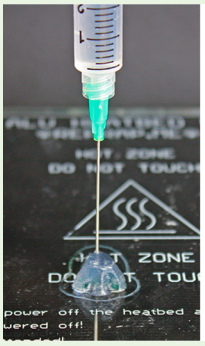

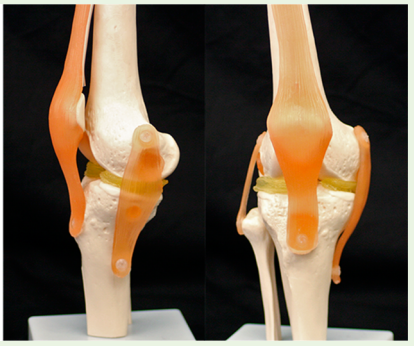

KEYWORDS: *tough hydrogel, double network hydrogel, 3D printing, tissue engineering*

1. INTRODUCTION

The meniscus, a network of tightly woven collagen fibers, serves as a shock absorber for the knee. A meniscal tear is among the most common knee injuries with more than 500,000 reported in the United States annually.[1] Serious tears in the meniscus often do not heal and require surgery to repair. For the most severe tears, the entire meniscus is removed in a process known as a meniscectomy.[2] Between 2005 and 2011, 387,000 meniscectomies were performed in the United States.[1]

If a patient who has previously lost a meniscus does begin to develop pain from early degeneration in the same knee compartment, he or she may be a candidate for meniscal replacement surgery.[3] Currently, the only FDA approved synthetic meniscus replacement product is NUSurface.[4] Though it provides mechanical support, its nonporous structure does not stimulate tissue regeneration, which could lead to failure over time due to wear, fatigue, or an adverse body response.[5,6] Two other meniscal replacement solutions that have undergone clinical trials, CMI and Actifit, do have the ability to stimulate tissue regeneration due to their porous nature, but this tissue is not the fibrocartilage that makes up the meniscus.[7−12] In addition, CMI and Actifit do not have the strength to serve as a total meniscus replacement and therefore have only been used as partial replacements in patients with some meniscus tissue remaining.[11]

Double network (DN) hydrogels may offer an innovative alternative to a meniscectomy by enabling the production of a customized synthetic meniscus. DN hydrogels are an extremely strong family of hydrogels that comprise two noncovalently bonded, interpenetrating polymer networks.[13] It has been shown that because of its unique porous and elastic structure, DN hydrogels stimulate articular cartilage regeneration.[14] As the meniscus acts as a buffer between two pieces of bone, any replacement should be able to withstand significant compressive stress with minimal distortion. A synthetic meniscus would ideally be custom-made for the patient and rapidly produced at relatively low cost, suggesting that 3D printing is a promising method for the production of synthetic menisci. Researchers have developed various approaches to 3D print hydrogel materials that are suitable for tissue engineering applications, including the use of liquid extrusion based 3D printing,[15−19] two-photon polymerization,[20] dynamic optical projection stereolithography,[21] and fused deposition modeling followed by cell culturing.[22,23] However, current 3D printable hydrogels do not meet the compression strength (14−59 MPa) required for replacing a human meniscus.

One approach to obtaining a 3D printable, tough hydrogel consists of using ionic cross-linking to reinforce the gel. Zhao et al. 3D printed a hybrid hydrogel made from a poly(ethylene glycol) diacrylate (PEGDA) network and alginate cross-linked by Ca^{2+}. This gel had a maximum fracture energy of 1500 J m^{-2}.[16] Spinks et al. used extrusion printing to produce a

Received: February 9, 2017
Accepted: April 2, 2017
Published: April 3, 2017

DOI: 10.1021/acsbiomaterials.7b00094
ACS Biomater. Sci. Eng. XXXX, XXX, XXX−XXX

polyacrylamide gel reinforced by an alginate-Ca^{2+} network; this gel had a toughness of 260 kJ m^{-3}.[24] Unfortunately, these 3D printable hydrogels disintegrate upon exposure to water because the calcium required for reinforcing the gel leaches out, making them unsuitable for *in vitro* and *in vivo* applications.

Another approach to 3D print a tough hydrogel is to print a gel with a temperature-dependent viscosity. Cong et al. used a 3D printer with a heated cartridge to print a polyacrylamide hydrogel reinforced with both agar and ionically cross-linked alginate at 45−60 °C.[19] Although they achieved a toughness of 3860 kJ m^{-3}, using a heated syringe increases the complexity of the printing process. Other strategies of reinforcing 3D printed hydrogels involve 3D printing a hydrogel-plastic composite[25] or encapsulating hydrogel in epoxy resin.[26]

In this article, we report the development of a shear-thinning ink that enables the printing of a DN hydrogel at room temperature. The concentration of Laponite, a layered silicate, and the molecular precursors of the first network were tuned to enable the ink to easily extrude through a fine nozzle but have sufficient viscosity after printing to retain the shape of a 3D printed object with a height up to 35 mm. Printing was performed with an easily modified $300 3D printer. After printing, objects were UV-cured, soaked in the precursor solution of the second network, and UV-cured again to form a DN hydrogel. The mechanical properties of the DN hydrogels can be tuned to have a compression strength approaching 100 MPa, double that of any previous 3D printed hydrogel. Objects printed with this gel retain their shape and mechanical integrity after soaking in water.

2. MATERIALS AND METHODS

2.1. Preparation of Hydrogel Precursor Solutions. Sodium 2-acrylamido-2-methylpropanesulfonate (AMPS), acrylamide, *N*,*N*′-methylenebis(acrylamide) (MBAA), and Irgacure 2959 (I2959) were purchased from Sigma-Aldrich. Laponite RDS was donated by BYK Additives and Instruments.

To make the 3D printable gel precursor, 1.0 g of Laponite RDS, 50 mg of I2959, and 60 mg of MBAA were dissolved in 8.1 g of water. The solution was allowed to stir overnight to homogenize, and 1.9 g of a 50 wt % AMPS solution was slowly added. The final concentrations of the components in the ink were 10 w/v % Laponite RDS, 0.40 M AMPS, 40 mM MBAA, and 22 mM I2959. The first network precursor was cured with a variable intensity UV transilluminator (VWR, 26XV).

The second network precursor was made by dissolving 14 wt % acrylamide (2.0 M), 0.01 wt % MBAA (0.64 mM), and 0.05 wt % (22 mM) I2959 in 10 g of water. After UV curing, the first network gel was soaked in the second network precursor for 24 h. The fully soaked gel was subsequently cured again with a variable intensity UV transilluminator (VWR, 26XV) in N_2 atmosphere. For the precursors with 4.0 and 6.0 M acrylamide, the concentration of I2959 was kept the same at 22 mM, and the molar ratio of acrylamide to MBAA was kept the same at ∼3125.

2.2. 3D Printing of the DN Hydrogel. To 3D print the DN hydrogel, a Reprap Prusa i3 3D printer was modified by replacing the thermoplastic filament extruder with a 3D printed syringe pump. The 3D model of the syringe pump is available for downloading at http://www.thingiverse.com/thing:1923150. A 5 mL syringe and a 21-gauge needle were used for extrusion. The first network precursor was loaded into the syringe and distributed to certain positions in 3D space according to a gcode file. After 3D printing, the printed object was cured with a variable intensity UV transilluminator (VWR, 26XV) for 10 min to 3 h, depending on the size of the hydrogel. Following the first UV curing step, the object was soaked in the second network precursor for 24 h, then cured again in a N_2 atmosphere for 30 min. To test the maximum height of 3D printed objects with this method, a 3D model of a 10 mm × 10 mm × 100 mm pillar was created and 3D printed. As the pillar increased in height during printing, the weight of the pillar caused it to compress. Compression of the pillar caused the distance between the needle and the pillar to increase until eventually (at a height of 35 mm) no additional gel could be extruded from the needle onto the pillar.

2.3. Mechanical Characterization. Dogbone-shaped samples were 3D printed according to ASTM D412 for tensile tests on a microstrain analyzer (TA Instrument, RSA III). The exact dimensions of samples were measured with a caliper before testing. Tensile tests were performed at a speed of 0.1 mm s^{-1}. The stress−strain curve between 0 and 10% strain was used to calculate the Young's modulus. Compression tests were performed on a materials testing machine (Instron, model 1321) on a speed of 0.1 mm s^{-1}. Cylindrical samples with a diameter of 10 mm and a height of 8 mm were 3D printed with the procedure described above. The exact sizes of samples were measured with a caliper before testing. The stiffness measurements were performed on a rheometer (TA Instrument, AR-G2). The stiffness data were extracted by linear regression of the stress−strain curve in the range of 0−10% strain. Viscosities of aqueous solutions of AMPS and Laponite RDS were measured on a rheometer (TA Instrument, AR-G2) with a 2° cone and plate geometry. Yield strain was determined with the 0.2% offset method. A line was drawn parallel to the linear part of the stress−strain curve, intersecting the "strain" axis at 0.2%. The yield strain was determined as the intersection of this line to the stress−strain curve.

3. RESULTS AND DISCUSSION

3.1. 3D Printing of Double Network Hydrogel. Figure 1 shows an overview of the steps for 3D printing a DN hydrogel.

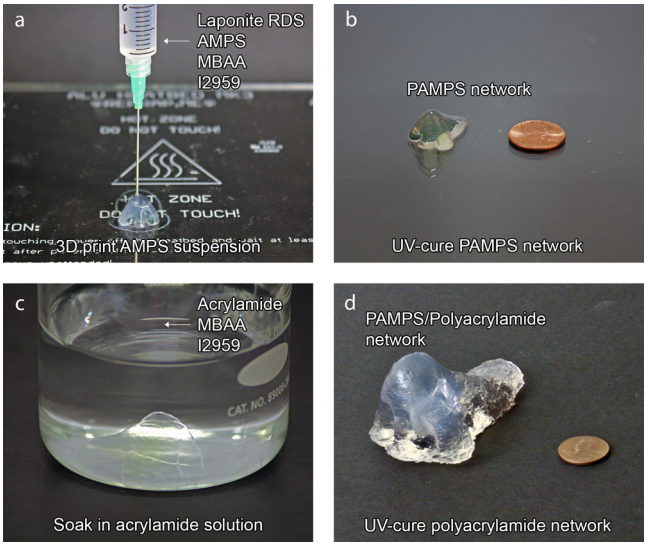

Figure 1. Steps for 3D printing a DN hydrogel: (a) 3D print the AMPS suspension; (b) UV-cure to obtain the PAMPS network; (c) soak the PAMPS network in an acrylamide solution; and (d) UV-cure to obtain a PAMPS/polyacrylamide double network.

A video (Movie S1) of gel printing is available in the Supporting Information. The process starts by 3D printing a suspension containing 10% w/v Laponite RDS, 0.40 M sodium 2-acrylamido-2-methylpropanesulfonate (AMPS), 40 mM *N*,*N*′-methylenebis(acrylamide) (MBAA), and 22 mM Irgacure 2959. Laponite RDS is a layered silicate rheology modifier that was added to control the viscosity of the ink, AMPS is the monomer for the first network hydrogel, MBAA is a cross-linker, and Irgacure 2959 is a photoinitiator for UV curing. After printing, the object was UV cured to form a stiff and brittle hydrogel consisting of poly(2-acrylamido-2-methylpro-

DOI: 10.1021/acsbiomaterials.7b00094
ACS Biomater. Sci. Eng. XXXX, XXX, XXX−XXX

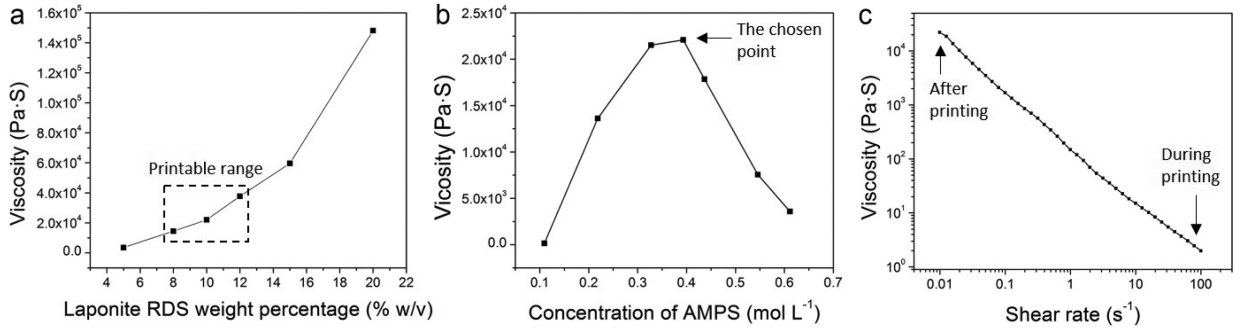

Figure 2. (a) Viscosity of aqueous solutions containing 0.40 M AMPS and different amounts of Laponite RDS. (b) Viscosity of aqueous solutions containing 10 w/v% Laponite RDS with different amounts of AMPS. (c) The viscosity of the 3D printable gel precursor as a function of shear rate.

panesulfonate), which is abbreviated as PAMPS. To improve its mechanical strength, a second interpenetrating network was created by soaking the first hydrogel network in an acrylamide solution, causing it to swell by 20%−750%. The swelling ratio is affected by the amount of MBAA in the first network, which in turn affects the stiffness of the gel. After soaking overnight, the fully swollen hydrogel was cured with UV light, forming a tough DN hydrogel consisting of an interpenetrating network of PAMPS and polyacrylamide. We note that both of these gels have been demonstrated to be biocompatible after the removal of the acrylamide monomer by dialysis.[14,27,28]

3.2. Optimizing the Viscosity of AMPS Solution for Printability. The 3D printed DN hydrogel described here was inspired by the PAMPS-polyacrylamide double network first reported by Gong et al.[13] However, in its original formulation this gel was not 3D printable. For 3D printing, the gel precursor should have a low viscosity during extrusion so that it can flow, and a high viscosity once extruded so that it can retain its shape. Since the viscosity of the first network precursor is too low to maintain a 3D structure after printing, the addition of a rheology modifier is necessary to enable the gel precursor to be 3D printed. The pH of solutions containing 2-acrylamido-2-methylpropanesulfonic acid (used in the original work by Gong et al.) are generally too low for thickening by most rheology modifiers such as layered silicates, alginate, or cellulose. Therefore, we replaced this acid with sodium 2-acrylamido-2-methylpropanesulfonate. Laponite RDS was then added to create a shear-thinning gel.[29] We note that Laponite RDS is a biocompatible material that is safe for food contact applications and thus should not compromise the biocompatibility of the PAMPS-polyacrylamide hydrogel.[29]

Figure 2a shows the effect of adding Laponite RDS to a solution of 0.40 M AMPS. Without Laponite, the viscosity of the AMPS solution is approximately equal to that of water (3.0 Pa·s). Addition of Laponite increases the viscosity from 3.5 kPa·s at 5 w/v % to 148.1 kPa·s at 20 w/v %. By 3D printing these different viscosities, we found that a viscosity of 14.48−37.72 kPa·s (8−12 w/v % Laponite) was sufficient to enable an object to retain its shape after extrusion without the frequent clogging of the nozzle that occurs if the viscosity is too high. The intermediate concentration of 10 w/v % Laponite RDS was chosen for all of the following printing experiments.

We also found that the concentration of the AMPS monomer has a strong effect on the viscosity of the 3D printable gel precursor. Changing the concentration of this precursor changes the ionic strength of the solution, which is known to affect the viscosity of a Laponite suspension.[29] We found that the viscosity was at a maximum with a concentration of 0.40 M AMPS. Although a higher concentration of AMPS would result in a gel with a higher strength, suspensions with higher concentrations of AMPS did not retain their shape after printing due to their lower viscosity. Therefore, for all of the following experiments we used a concentration of 0.40 M AMPS in the 3D printed gel precursor.

Figure 2c demonstrates the shear-thinning properties of a solution containing 10 w/v % Laponite RDS and 0.40 M AMPS. When the suspension is extruded at a speed of 5.0 mm s^{-1}, its shear rate can be calculated with the following formula, wherein $\dot{\gamma}$ is the shear rate, ν is the linear flow rate of fluid in the nozzle, and d is the inside diameter of the needle:[30]

$$\dot{\gamma} = \frac{8\nu}{d} = \frac{8 \times 5.0\ \text{mm s}^{-1}}{0.514\ \text{mm}} = 78\ \text{s}^{-1}$$

At this shear rate, the low viscosity of the suspension allows it to be easily extruded. As soon as the gel precursor leaves the nozzle, it reverts to the high viscosity state, and the lack of fluid flow enables the printing of the liquid in a wide variety of shapes, with heights up to ∼35 mm.

3.3. 3D Printing of the DN Hydrogel. The rheological properties of the gel precursor ink allow it to be printed with most liquid extrusion-based 3D printers, such as those that use a syringe or air pressure to dispense a liquid solution. For this work, we used a modified Prusa i3 3D printer available for about $300 (see Figure S1). We replaced the original polymer extruder with a syringe-based extruder consisting of 3D printed parts and a lead screw stepper motor.[31] Conventional 3D modeling software (Tinkercad, Autodesk 123D) was used to design the objects, and these shapes were converted to gcode files for 3D printing using Cura as the slicing program.

Figure 3 demonstrates the 3D printing of menisci with the DN hydrogel. In Figure 3a, a 3D model of a pair of menisci was obtained by scanning an anatomical model of a human knee with X-ray computed tomography. A pair of artificial menisci was then 3D printed based on that 3D model and put back into the same knee model as a replacement. Since it was obtained from the original menisci shape, the 3D printed meniscus fits the model joint perfectly with no modifications after printing. We imagine a similar workflow could potentially be used for real patients, in which 3D images of their menisci served as the starting point for creating a replacement. In contrast, partial synthetic meniscus replacements such as CMI and Actifit are not customized for each patient but are instead trimmed from a standard shape by hand using a scalpel.[32,33] The whole meniscus replacement product NUSurface also comes in seven standard sizes that are not customizable, and finding

DOI: 10.1021/acsbiomaterials.7b00094
ACS Biomater. Sci. Eng. XXXX, XXX, XXX−XXX

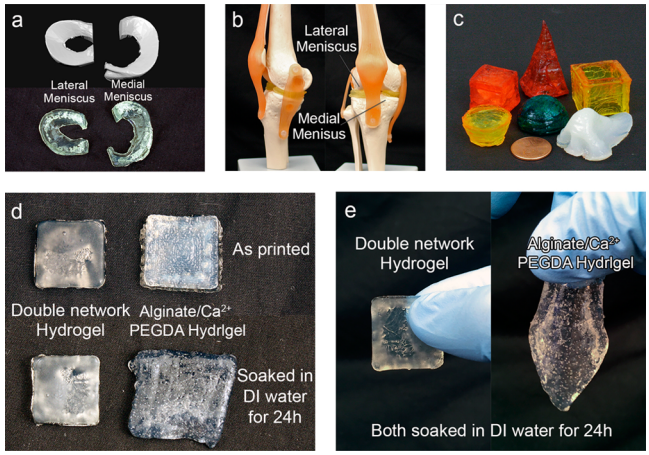

Figure 3. (a) Top: 3D model of a pair of menisci. Bottom: 3D printed DN hydrogel menisci. The 3D model was obtained by scanning an anatomical model of a human knee with a high resolution X-ray computed tomography scanner (MicroCT). (b) The 3D printed menisci in the knee model. (c) Front row: a reverse cone (yellow), a hemisphere (green), and a human nose scan (off-white). Back row: a cube (red), a sharp pyramid (red), and a square tube (yellow). Food coloring was added to make the originally transparent gels more visible. (d) The 3D printed hydrogel from this work (left) retains its shape after soaking in DI water for 24 h, while a 3D printed PEGDA + alginate/Ca^{2+} semi-interpenetrating hydrogel swells. (e) A piece of 3D printed double network hydrogel retains its shape when held, but the 3D printed PEGDA hydrogel was deformed by gravity.

the right size can involve some trial and error during surgery.[4,34,35]

Figure 3c shows a series of objects to demonstrate that a variety of geometries can be printed with the shear-thinning gel precursor. The thin pyramid demonstrates printing of objects with high vertical aspect ratios. The reverse cone demonstrates printing of an overhang. The human nose demonstrates the ability to print complex anatomical structures that combine the need to print a high vertical aspect ratio and overhangs. The minimum spacing between printed lines (Figure S2) that could be achieved with a needle diameter of 500 μm without the lines touching was 750 μm, demonstrating that minimal spreading occurs after printing of the ink. This resolution can likely be improved by using a needle with a smaller diameter.

After soaking in the second network precursor, the printed first network swells and exhibits a volume increase of 20%–750%. This swelling is isotropic, and the degree of swelling must be taken into account when designing an object with a desired size. Swelling decreases the resolution and minimum feature size that can be printed for a given needle diameter. The degree of swelling depends largely on the concentration of MBAA in the first network; a higher concentration of MBAA in the first network leads to less swelling because of the increase in stiffness with higher concentrations of MBAA. Thus, swelling can be minimized at high MBAA concentrations.

In order to be used *in vivo*, a gel-based meniscus should not lose its shape and strength after prolonged soaking in water. In Figure 3d, we compare the shape of the DN gel to a previously reported PEGDA + alginate/Ca^{2+} semi-interpenetrating hydro-

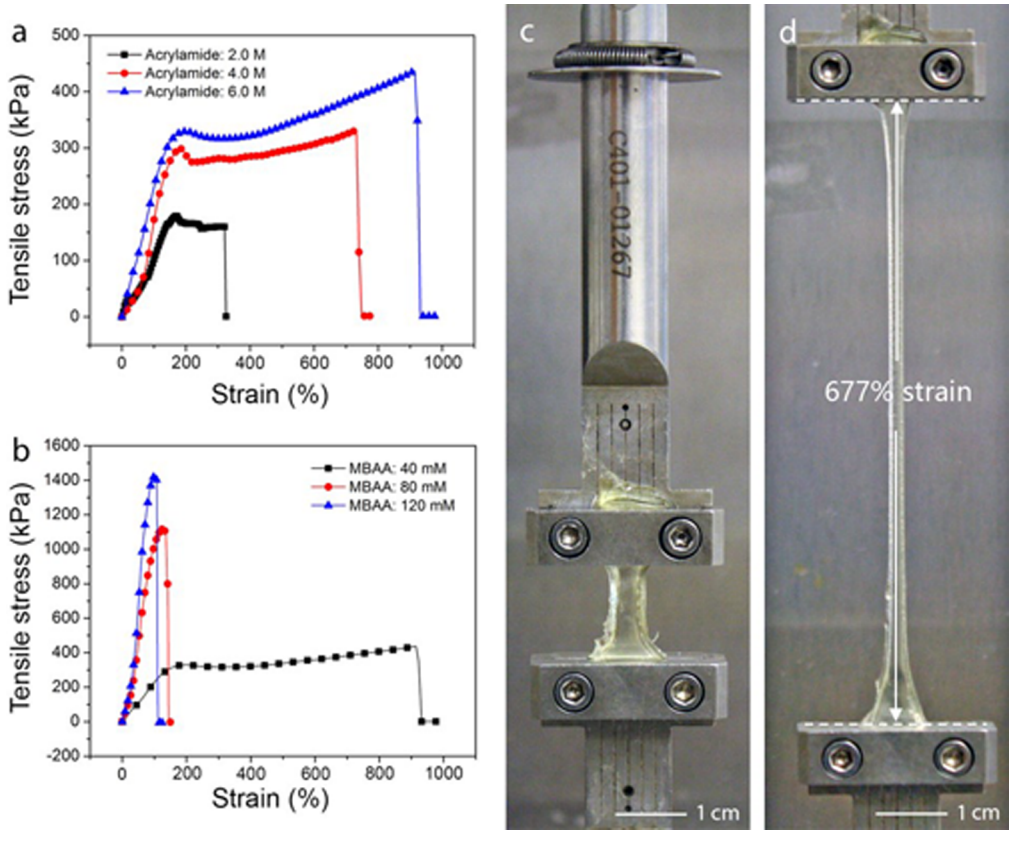

Figure 4. (a) Tensile stress–strain curve of samples with 40 mM MBAA in the first network and different concentrations of acrylamide in the second network. (b) Tensile stress–strain curve of samples with different concentrations of MBAA in the first network and 6.0 M acrylamide in the second network. (c,d) A dogbone with 40 mM MBAA and 6.0 M acrylamide before and after stretching to 677% strain.

DOI: 10.1021/acsbiomaterials.7b00094
ACS Biomater. Sci. Eng. XXXX, XXX, XXX–XXX

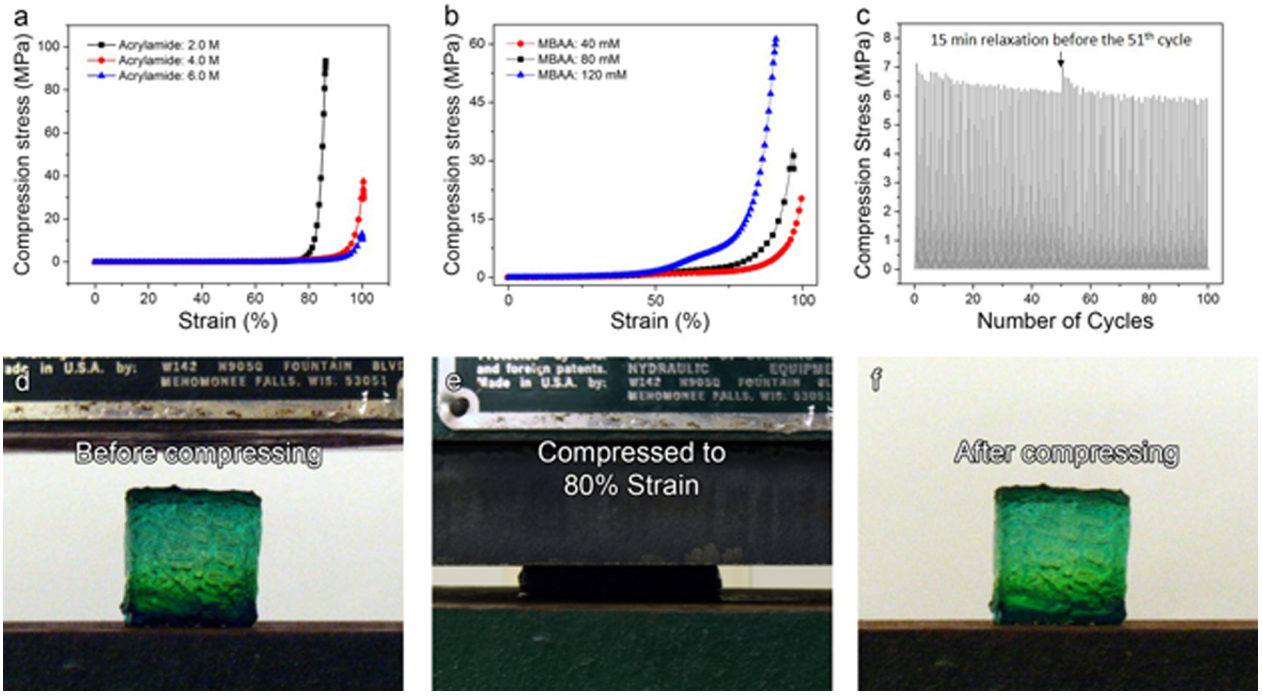

Figure 5. (a) Compression stress−strain curves of DN hydrogels made with 40 mM MBAA and varying concentrations of acrylamide. (b) Compression stress−strain curves of DN hydrogels made with 6.0 M of acrylamide and varying amounts of MBAA. (c) Compression stress for a DN hydrogel with 120 mM MBAA and 6.0 M acrylamide at a strain of 75% strain over 100 cycles. The gel was relaxed at cycle 50 for 15 min. (d−f) A piece of cubic DN hydrogel before, during, and after being compressed to 80% strain.

gel.[16] There is no observable change in the shape of the DN gel after immersion in DI water for 24 h, but the PEGDA-based gel clearly deforms as the Ca^{2+} leaches into solution. In Figure 3e, both the DN gel and the PEGDA + alginate/Ca^{2+} gel was soaked in DI water for 24 h, then suspended by hand. While the DN hydrogel retained its stiffness after the 24-h soak, the PEGDA + alginate/Ca^{2+} gel was immediately deformed by gravity.

3.4. Tensile Characteristics of the DN Hydrogel. The mechanical properties of the 3D-printable DN hydrogel could be tuned by changing the concentration of the cross-linker, MBAA, in the first network or the concentration of acrylamide in the second network while keeping the molar ratio of acrylamide to MBAA in the second network constant at 3125:1. Figure 4a shows that increasing the concentration of acrylamide in the second network from 2.0 to 6.0 M increases the maximum elongation strain from 322% to 923%, with a concurrent increase in toughness from 404.1 kJ m^{-3} to 3024 kJ m^{-3}. This toughness is similar to the best result previously reported (3860 kJ m^{-3}) that relied on an alginate network.[19] The yield strain of all samples shown in Figure 4a and b is listed in Table S1.

Although increasing the acrylamide concentration leads to excellent toughness, the elastic modulus and tensile strength may not be sufficient for some applications. Therefore, we also explored the effect of the cross-linker, MBAA, on the stiffness of the PAMPS-polyacrylamide DN hydrogel. Figure 4b demonstrates that the elastic modulus of the DN hydrogel with 120 mM MBAA is 1060 kPa, which is 449% greater than that of the DN hydrogel with 40 mM MBAA. Both of these gels were made with 6.0 M of acrylamide in the second network. More MBAA in the first network also decreases the maximum elongation from 923% to 112%. Thus, tuning the MBAA cross-linker concentration allows one to tune the gel to exhibit a desired trade-off between stiffness and maximum elongation. The increase in stiffness that results from increasing the amount of MBAA also affects the swelling behavior of the first network during immersion in the second network precursor solution. Hydrogels with 40 mM MBAA exhibited a volume increase of 650% during the soaking step, but the swelling ratio of hydrogels with 120 mM MBAA was less than 120%.

Previous research has shown that the toughness of the DN hydrogel is related to local yielding effects.[36] When stretched over the yield strain, the brittle first network fractures and dissipates energy. This phenomenon can be seen in a comparison of the stress−strain curves that show the first and second cycle of tensile testing (Figure S3). After the first cycle, it is thought that the fracture of the first network creates a less stiff, sliding-ring hydrogel with different stress−strain characteristics.[37] These results show that the 3D printed DN hydrogel reported here has similar mechanical properties as previously reported PAMPS-polyacrylamide DN hydrogels, despite the modifications made to make it 3D printable.

3.5. Compression Characteristics of DN Hydrogel. Compression tests were performed on the 3D printed gels to determine their suitability for the replacement of meniscus cartilage. Figure 5a and b shows that a DN hydrogel with 40 mM MBAA in the first network and 2.0 M acrylamide in the second network has the biggest compression fracture strength of 93.5 MPa. Increasing the concentration of acrylamide increases the stiffness of the gel in the low-strain region, while leading to a lower maximum stress in the high-strain region. The compression strength of the DN hydrogel decreased from 93.5 to 10.5 MPa when the acrylamide concentration was increased from 2.0 to 6.0 M. Higher compression strengths can be obtained without a loss of ductility by increasing the concentration of MBAA in the first network. When the MBAA concentration was increased from 40 to 120 mM in the first

DOI: 10.1021/acsbiomaterials.7b00094
ACS Biomater. Sci. Eng. XXXX, XXX, XXX−XXX

Table 1. Mechanical Properties of Bovine Cartilage and 3D Printed Hydrogels

	compression strength (MPa)	tensile strength (MPa)	elastic modulus (MPa)		toughness (kJ m^{-3})
			tensile	compression	
bovine cartilage[38,40,41]	14−59	0.53−9	10.1−28.3	0.31	
polyacrylamide-alginate + Ca^{2+}[24]		0.17	0.066		260
agar-polycrylamide-alginate + Ca^{2+}[19,42]	40	0.781	0.810		3860
40 mM MBAA, 2.0 M acrylamide	**93.5**	0.160	0.069	0.051	401.4
40 mM MBAA, 6.0 M acrylamide	17.9	0.437	0.167	0.11	**3024**
120 mM MBAA, 6.0 M acrylamide	**61.9**	**1.417**	1.016	**0.44**	1060

network and the acrylamide concentration was kept at 6.0 M, the compression strength increased from 10.5 to 61.9 MPa, while retaining a maximum strain of 99%. If the MBAA concentration was further increased to 140 mM, the gel became more brittle and fractured at a strain of 75%, leading to a decreased compression strength of 5.05 MPa.

In Figure 5d−f, a 3D printed cube of DN gel with 40 mM MBAA in the first network and 6.0 M acrylamide in the second network was compressed to 80% strain, then released, showing no visible sign of plastic deformation after compression. To further test the fatigue resistance of the DN hydrogel material, a cylindrical DN hydrogel sample was compressed to a strain of 75% with a rate of 1 mm s^{-1}, the position was held for 1 s, and the gel was released back to its original height at a speed of 1 mm s^{-1}. After the first 50 cycles, the maximum stress in each cycle decreased from 7.12 to 6.14 MPa. In order to determine if the softening effect was reversible, the sample was rested for 15 min before being compressed for another 50 cycles. As shown in Figure 5c, the maximum stress recovered to a value of 7.01 MPa after relaxation, which indicates that the loss of strength of the DN hydrogel is temporary. After the 60th cycle, the stress plateaued at 5.87 MPa, showing only some fluctuations. The softening is likely due to the fact that the gel requires several minutes before it goes to back to its original height. After the first compression cycle, the total height of the gel is slightly smaller than it was originally, but the original height was still used for the strain calculation. This results in the gel being compressed to a strain several percent smaller than 75%, leading to a smaller stress.

3.6. Comparison of 3D Printed Tough Hydrogels and Bovine Cartilage. Table 1 compares the various mechanical properties of bovine articular cartilage, previously reported 3D printed hydrogels, and several optimized gels in this work. By tuning the formula of the 3D printed DN hydrogel, the mechanical properties can be tuned to surpass those of most other gels. The 3D printed gel with 120 mM MBAA in the first network and 6.0 M acrylamide in the second network was found to be the best potential meniscus replacement (see Figure S4 and Figure 5b) due to its excellent stiffness (0.44 MPa compared to 0.31 MPa of bovine femur cartilage) and compression strength (61.9 MPa compared to 14−59 MPa of bovine cartilage).[38,39] Although a further increase of the MBAA concentration in the first network increases the stiffness of the 3D printed gels, it causes the gel to be brittle and ultimately lowers the compression strength.

4. CONCLUSIONS

In conclusion, this paper introduces a method to 3D print double network hydrogels that have a compression strength, tensile strength, and elastic modulus greater than any previous 3D printed gels. Tuning the ratio of the cross-linker in the first network to the acrylamide monomer in the second network allowed for the formulation of a gel with a compression strength and stiffness greater than that of bovine cartilage. In addition, the DN hydrogels could be printed at room temperature with a modified $300 3D printer and exhibited no deformation after soaking in water for 24 h. This new gel presents an opportunity to customize hydrogel implants based on X-ray computed tomography images of a patient's own anatomy. Future work may examine the relationship between the mechanical properties of this printed gel and its potential to stimulate cartilage tissue growth.

■ ASSOCIATED CONTENT

Supporting Information

The Supporting Information is available free of charge on the ACS Publications website at DOI: 10.1021/acsbiomaterials.7b00094.

Picture of a $300 3D printer; photo of the printing resolution test; tensile stress−strain curve; effect of MBAA concentration in the first network on the compression strength and stiffness of hydrogels; and tensile yield strain of double network hydrogels (PDF)

A video of gel printing (AVI)

■ AUTHOR INFORMATION

Corresponding Author

*Department of Chemistry, Duke University, 124 Science Drive, Box 90354, Durham, NC 27708, United States. E-mail: Benjamin.wiley@duke.edu.

ORCID

Feichen Yang: 0000-0002-6008-0247

Benjamin J. Wiley: 0000-0003-0055-9018

Funding

This work was supported in part by start-up funds from Duke University, NSF Grant No. ECCS-1344745, and an NSF CAREER award (DMR-1253534).

Notes

The authors declare no competing financial interest.

■ ACKNOWLEDGMENTS

We acknowledge the assistance of Dr. Richard Glisson (Duke University Medical Center, Duke University) for the compression testing experiments.

■ REFERENCES

(1) Abrams, G. D.; Frank, R. M.; Gupta, A. K.; Harris, J. D.; McCormick, F. M.; Cole, B. J. Trends in meniscus repair and meniscectomy in the United States, 2005−2011. *Am. J. Sport. Med.* **2013**, *41*, 2333−2339.

(2) DEHAVEN, K. E. Decision-making factors in the treatment of meniscus lesions. *Clin. Orthop. Relat. Res.* **1990**, *252*, 49−54.

DOI: 10.1021/acsbiomaterials.7b00094
ACS Biomater. Sci. Eng. XXXX, XXX, XXX−XXX

(3) McDermott, I. Meniscal tears, repairs and replacement: their relevance to osteoarthritis of the knee. *Br. J. Sports Med.* **2011**, *45*, 292−297.
(4) NUsurface® Meniscus Implant. https://activeimplants.com/products/nusurface-meniscus-implant/ (accessed Dec 20, 2016).
(5) Hollister, S. J. Porous scaffold design for tissue engineering. *Nat. Mater.* **2005**, *4*, 518−524.
(6) Vrancken, A. C. T.; Buma, P.; van Tienen, T. G. Synthetic meniscus replacement: a review. *Int. Ortho.* **2013**, *37*, 291−299.
(7) What is Actifit®-Actifit. http://actifit.info/what-is-actifit/ (accessed Dec 20, 2016).
(8) Stone, K. R.; Rodkey, W. G.; Webber, R.; McKinney, L.; Steadman, J. R. Meniscal regeneration with copolymeric collagen scaffolds In vitro and in vivo studies evaluated clinically, histologically, and biochemically. *Am. J. Sport. Med.* **1992**, *20*, 104−111.
(9) Maher, S. A.; Rodeo, S. A.; Doty, S. B.; Brophy, R.; Potter, H.; Foo, L.-F.; Rosenblatt, L.; Deng, X.-H.; Turner, A. S.; Wright, T. M. Evaluation of a porous polyurethane scaffold in a partial meniscal defect ovine model. *Arthroscopy* **2010**, *26*, 1510−1519.
(10) Collagen Meniscus Implant. http://www.ivysportsmed.com/en/collagen-meniscus-implant (accessed Dec 20, 2016).
(11) Welsing, R. T.; van Tienen, T. G.; Ramrattan, N.; Heijkants, R.; Schouten, A. J.; Veth, R. P.; Buma, P. Effect on Tissue Differentiation and Articular Cartilage Degradation of a Polymer Meniscus Implant A 2-Year Follow-up Study in Dogs. *Am. J. Sports. Med.* **2008**, *36*, 1978−1989.
(12) Spencer, S.; Saithna, A.; Carmont, M.; Dhillon, M.; Thompson, P.; Spalding, T. Meniscal scaffolds: early experience and review of the literature. *Knee* **2012**, *19*, 760−765.
(13) Gong, J. P.; Katsuyama, Y.; Kurokawa, T.; Osada, Y. Double-network hydrogels with extremely high mechanical strength. *Adv. Mater.* **2003**, *15*, 1155−1158.
(14) Yasuda, K.; Kitamura, N.; Gong, J. P.; Arakaki, K.; Kwon, H. J.; Onodera, S.; Chen, Y. M.; Kurokawa, T.; Kanaya, F.; Ohmiya, Y. A Novel Double-Network Hydrogel Induces Spontaneous Articular Cartilage Regeneration in vivo in a Large Osteochondral Defect. *Macromol. Biosci.* **2009**, *9*, 307−316.
(15) Kolesky, D. B.; Truby, R. L.; Gladman, A. S.; Busbee, T. A.; Homan, K. A.; Lewis, J. A. 3D Bioprinting of Vascularized, Heterogeneous Cell-Laden Tissue Constructs. *Adv. Mater.* **2014**, *26*, 3124−3130.
(16) Hong, S.; Sycks, D.; Chan, H. F.; Lin, S.; Lopez, G. P.; Guilak, F.; Leong, K. W.; Zhao, X. 3D printing of highly stretchable and tough hydrogels into complex, cellularized structures. *Adv. Mater.* **2015**, *27*, 4035−4040.
(17) Bertassoni, L. E.; Cardoso, J. C.; Manoharan, V.; Cristino, A. L.; Bhise, N. S.; Araujo, W. A.; Zorlutuna, P.; Vrana, N. E.; Ghaemmaghami, A. M.; Dokmeci, M. R. Direct-write bioprinting of cell-laden methacrylated gelatin hydrogels. *Biofabrication* **2014**, *6*, 024105.
(18) Hinton, T. J.; Jallerat, Q.; Palchesko, R. N.; Park, J. H.; Grodzicki, M. S.; Shue, H.-J.; Ramadan, M. H.; Hudson, A. R.; Feinberg, A. W. Three-dimensional printing of complex biological structures by freeform reversible embedding of suspended hydrogels. *Sci. Adv.* **2015**, *1*, e1500758.
(19) Wei, J.; Wang, J.; Su, S.; Wang, S.; Qiu, J.; Zhang, Z.; Christopher, G.; Ning, F.; Cong, W. 3D printing of an extremely tough hydrogel. *RSC Adv.* **2015**, *5*, 81324−81329.
(20) Hahn, M. S.; Miller, J. S.; West, J. L. Three-dimensional biochemical and biomechanical patterning of hydrogels for guiding cell behavior. *Adv. Mater.* **2006**, *18*, 2679−2684.
(21) Zhang, A. P.; Qu, X.; Soman, P.; Hribar, K. C.; Lee, J. W.; Chen, S.; He, S. Rapid Fabrication of Complex 3D Extracellular Microenvironments by Dynamic Optical Projection Stereolithography. *Adv. Mater.* **2012**, *24*, 4266−4270.
(22) Kang, H.-W.; Lee, S. J.; Ko, I. K.; Kengla, C.; Yoo, J. J.; Atala, A. A 3D bioprinting system to produce human-scale tissue constructs with structural integrity. *Nat. Biotechnol.* **2016**, *34*, 312−319.
(23) Jakus, A. E.; Rutz, A. L.; Jordan, S. W.; Kannan, A.; Mitchell, S. M.; Yun, C.; Koube, K. D.; Yoo, S. C.; Whiteley, H. E.; Richter, C.-P. Hyperelastic "bone": A highly versatile, growth factor−free, osteogenerative, scalable, and surgically friendly biomaterial. *Sci. Transl. Med.* **2016**, *8*, 358ra127−358ra127.
(24) Bakarich, S. E.; Beirne, S.; Wallace, G. G.; Spinks, G. M. Extrusion printing of ionic−covalent entanglement hydrogels with high toughness. *J. Mater. Chem. B* **2013**, *1*, 4939−4946.
(25) Zhao, X. Multi-scale multi-mechanism design of tough hydrogels: building dissipation into stretchy networks. *Soft Matter* **2014**, *10*, 672−687.
(26) Bakarich, S. E.; Gorkin, R., III; in het Panhuis, M.; Spinks, G. M. Three-dimensional printing fiber reinforced hydrogel composites. *ACS Appl. Mater. Interfaces* **2014**, *6*, 15998−16006.
(27) Barry, R. A.; Shepherd, R. F.; Hanson, J. N.; Nuzzo, R. G.; Wiltzius, P.; Lewis, J. A. Direct-Write Assembly of 3D Hydrogel Scaffolds for Guided Cell Growth. *Adv. Mater.* **2009**, *21*, 2407−2410.
(28) Narita, T.; Ohtakeyama, R.; Matsukata, M.; Gong, J.; Osada, Y. Kinetic study of cell disruption by ionic polymers with varied charge density. *Colloid Polym. Sci.* **2001**, *279*, 178−183.
(29) Laponite RDS Data sheet. http://www.additives-downloads.de/output/ag_download.aspx?file=PB%20Laponite%20RDS_EN.pdf (accessed April 6, 2017).
(30) Darby, R. *Chemical Engineering Fluid Mechanics, Revised and Expanded*; Taylor & Francis: Abington, 2001; p 64.
(31) Syringe Pump. http://www.thingiverse.com/thing:1923150 (accessed Nov 28, 2016).
(32) CMI Surgery. http://www.ivysportsmed.com/en/collagen-meniscus-implant/receiving-cmi/cmi-surgery (accessed Dec 22, 2016).
(33) Actifit® Procedure-Actifit. http://actifit.info/patient-centre/actifit-procedure/ (accessed Dec 22, 2016).
(34) Farr, J.; Gomoll, A. *Cartilage Restoration: Practical Clinical Applications*; 1st ed.; Springer-Verlag: New York, 2014; pp 237.
(35) Parker, D. *Management of Knee Osteoarthritis in the Younger, Active Patient*; Springer: New York, 2016; pp 151−152.
(36) Gong, J. P. Why are double network hydrogels so tough? *Soft Matter* **2010**, *6*, 2583−2590.
(37) Yasuda, K.; Gong, J. P.; Katsuyama, Y.; Nakayama, A.; Tanabe, Y.; Kondo, E.; Ueno, M.; Osada, Y. Biomechanical properties of high-toughness double network hydrogels. *Biomaterials* **2005**, *26*, 4468−4475.
(38) Schinagl, R. M.; Gurskis, D.; Chen, A. C.; Sah, R. L. Depth-dependent confined compression modulus of full-thickness bovine articular cartilage. *J. Orthop. Res.* **1997**, *15*, 499−506.
(39) Korhonen, R.; Laasanen, M.; Töyräs, J.; Rieppo, J.; Hirvonen, J.; Helminen, H.; Jurvelin, J. Comparison of the equilibrium response of articular cartilage in unconfined compression, confined compression and indentation. *J. Biomech.* **2002**, *35*, 903−909.
(40) Kerin, A.; Wisnom, M.; Adams, M. The compressive strength of articular cartilage. *Proc. Inst. Mech. Eng., Part H* **1998**, *212*, 273−280.
(41) Williamson, A. K.; Chen, A. C.; Masuda, K.; Thonar, E. J.; Sah, R. L. Tensile mechanical properties of bovine articular cartilage: variations with growth and relationships to collagen network components. *J. Orthop. Res.* **2003**, *21*, 872−880.
(42) Chen, Q.; Zhu, L.; Zhao, C.; Wang, Q.; Zheng, J. A Robust, One-Pot Synthesis of Highly Mechanical and Recoverable Double Network Hydrogels Using Thermoreversible Sol-Gel Polysaccharide. *Adv. Mater.* **2013**, *25*, 4171−4176.

DOI: 10.1021/acsbiomaterials.7b00094
ACS Biomater. Sci. Eng. XXXX, XXX, XXX−XXX